Functional Differences of Photosystem II from *Synechococcus elongatus* and Spinach Characterized by Flash Induced Oxygen Evolution Patterns†

Sabina Isgandarova,‡ Gernot Renger,§ and Johannes Messinger*,‡

Max Planck Institute for Bioinorganic Chemistry, Postfach 101365, D-45413 Mülheim an der Ruhr, Germany, and Max-Volmer Laboratorium für Physikalische Chemie der TU Berlin, PC 14, Strasse des 17. Juni 135, D-10623 Berlin, Germany

Received May 7, 2003; Revised Manuscript Received June 4, 2003

ABSTRACT: Detailed comparative studies of flash induced oxygen evolution patterns in thylakoids from the thermophilic cyanobacterium *Synechococcus elongatus* (*S. elongatus;* also referred to as *Thermosynechococcus elongatus*) and from spinach led to the following results: (i) the miss parameter α of *S. elongatus* thylakoids exhibits a pronounced temperature dependence with a minimum of 7% at 25 °C and values of 17 and 10% at 3 and 35 °C, respectively, while for spinach thylakoids α decreases continuously from 18% at 35 °C down to 8% at 3 °C; (ii) at all temperatures, the double hit probability β exceeds in *S. elongatus* the corresponding values of spinach by an increment $\Delta\beta$ of about 3%; (iii) at 20 °C the slow relaxation of the oxidation states S_2 and S_3 is about 15 and 30 times, respectively, slower in *S. elongatus* than in spinach, while the reduction of these S states by tyrosine Y_D is 2−3 times faster; (iv) the reaction $S_0Y_D^{ox} \rightarrow S_1Y_D$ is slower by a factor of 4 in *S. elongatus* as compared to spinach; and (v) the activation energies of S state dark relaxations in *S. elongatus* are all within a factor of 1.5 as compared to the previously reported values from spinach thylakoids [Vass, I., Deak, Z., and Hideg, E. (1990) *Biochim. Biophys. Acta 1017,* 63−69; Messinger, J., Schröder, W. P., and Renger, G. (1993) *Biochemistry 32,* 7658−7668], but the difference between the activation energies of the slow S_2 and S_3 decays is significantly larger in *S. elongatus* than in spinach. These results are discussed in terms of differences between cyanobacteria and higher plants on the acceptor side of PSII and a shift of the redox potential of the couple Y_D/Y_D^{ox}. The obtained data are also suitable to address questions about effects of the redox state of Y_D on the miss probability and the possibility of an S state dependent miss parameter.

In all oxygenic photosynthetic organisms (cyanobacteria, green algae, higher plants), the oxidation of water to molecular oxygen and four protons takes place in the oxygen evolving complex (OEC) that is a functional part of photosystem II (PSII)[1] (for review, see refs *1*−*5*). PSII is a membrane-bound multimeric pigment−protein complex of about 30 subunits (*6*). Recently, great progress has been achieved in unraveling structural features and the spatial arrangement of its cofactors by crystallization of PSII core complexes from the thermophilic cyanobacteria *Synechococcus elongatus naegeli* (*S. elongatus*; also referred to as *Thermosynechococcus elongatus BP1*) (*7*) and *Synechococcus vulcanus* (*S. vulcanus*; also referred to as *Thermosynechococcus vulcanus*) (*8*) by X-ray structure analysis to 3.8 and 3.7 Å resolution, respectively. These results confirm that all known cofactors for electron transport in PSII are bound by the D1 and D2 polypeptides located in the inner core of the PSII complex.

The OEC is comprised of a Mn_4O_xCa complex, its ligands (including water), and tyrosine Y_Z of polypeptide D1 (*1*−*5*). Other ions such as Cl^- and HCO_3^- (*9*−*13*) are also discussed as cofactors, but so far no sound proof for binding at or near the Mn_4O_xCa complex could be provided. In fact, it was recently shown that Cl^- most likely does not bind to the Mn_4O_xCa complex but is involved in a proton relay network from the OEC to the lumen (*14*). Photosynthetic water cleavage is energetically driven by the strongly oxidizing cation radical $P680^{+\bullet}$ that is generated as a result of the light induced charge separation (for review, see ref *15*). $P680^{+\bullet}$ oxidizes Y_Z to Y_Z^{ox}, which in turn oxidizes the Mn_4O_xCa complex. In this way, the OEC is driven through a redox cycle, in which the five intermediates are referred to as S_i states ($i = 0, ..., 4$) (*16*).

After sufficiently long dark-adaptation, essentially all OEC attain the S_1 state. The S_2 and S_3 states are reduced in the dark by both tyrosine Y_D of polypeptide D2 (fast phase) and more slowly by components of the acceptor side such as Q_B^- (*17*−*20*). In contrast, S_0 is slowly oxidized by Y_D^{ox} to the dark-stable S_1 state (*19*−*23*). In Scheme 1, the S_4 state is thought to be unstable and to rapidly decay under the

† Financial support from DFG project Me 1629/2-2 and the MPG is gratefully acknowledged.

* Corresponding author. E-mail: messinger@mpi-muelheim.mpg.de. Telephone: + 49 208 306 3865. Fax: + 49 208 306 3951.

‡ Max Planck Institute for Bioinorganic Chemistry.

§ Max-Volmer Laboratorium für Physikalische Chemie der TU Berlin.

[1] Abbreviations: α and β, miss and double hit probabilities during flash induced oxygen evolution, respectively; Chl, chlorophyll; EPR, electron paramagnetic resonance; Hepes, (*N*-[2-hydroxyethyl]piperazine-*N*′-[2-ethanesulfonic acid]); FIOPs, flash induced oxygen evolution patterns; OEC, oxygen evolving complex; PSII, photosystem II; S states, S_{-5}, ..., S_4 oxidation states of the OEC; Y_D, redox active tyrosine 160 of the D2 polypeptide of PSII; Y_Z, redox active tyrosine 161 of the D1 polypeptide of PSII.

10.1021/bi034744b CCC: $25.00
Published on Web 07/10/2003

Scheme 1: Kok Model for S State Advancement during Oxygen Evolution (*16*)

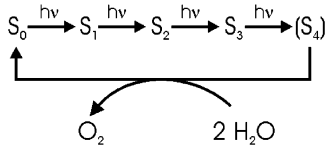

release of molecular oxygen into the S_0 state. The S states were found to be paramagnetic. The S_2 state exhibits an EPR multiline signal at $g = 2$ (*24*) and an alternate signal at $g = 4.1$ (*25*, *26*). The S_0 state is detectable in the presence of low concentrations of methanol (*27*−*29*). Using parallel polarization, EPR signals were also discovered for S_1 and S_3 states (*30*−*34*).

Important insights into the mechanism of photosynthetic water oxidation can be gathered from flash induced oxygen evolution patterns (FIOPs), in which PSII samples are illuminated with a train of saturating single turnover flashes. The high S_1 population in well dark-adapted samples leads to a pronounced first burst of oxygen evolution after the third flash, and further maxima occur with a damped period four oscillation until each flash gives identical yields. The damping originates from the fact that in each flash a fraction of OEC is not oxidized (miss probability, α), while depending on the flash profile a small percentage of other OEC can be oxidized twice (double hit probability, β). The origins of the parameters α and β are quite different. The double hit probability can be practically eliminated by using short enough actinic flashes (*35*), while the parameter α is an intrinsic property of PSII. The magnitude of α is expected to depend on redox equilibria between cofactors of the donor and the acceptor sides of PSII (*36*−*38*). Therefore, it is clear that the assumption of S state independent misses is an oversimplification. However, the precise S state dependencies of the miss and double hit probabilities are difficult to measure, and equal misses and double hits have been proven to be good approximations for most purposes (*16*). Additional S states of the OEC are accessible by incubation of PSII with low concentrations of reductants such as hydrazine and hydroxylamine (for review, see ref *39*) and are postulated as intermediates (*40*, *41*) in the process of photoactivation of the OEC (*42*, *43*). The lowest oxidation state clearly identified so far is the S_{-3} state (*44*), but preliminary data have been presented that support the existence of labile S_{-4} and S_{-5} states (*45*).

Since the crystal structure of PSII is available only for the thermophilic cyanobacteria *S. elongatus* (*7*) and *S. vulcanus* (*8*), which grow at about 55 °C, it is important to investigate whether functional and structural differences exist between *S. elongatus* and the generally better studied plant PSII from spinach. Earlier studies have shown that the kinetics of S state transitions and their activation energies are surprisingly similar in these different organisms (*46*, *47*). Likewise, on the basis of EPR and EXAFS studies the structure of the Mn_4O_xCa complex is very similar in the two systems (*48*−*51*). On the other hand, also some differences have been reported: (i) a greater stability of the S_2 and S_3 states in whole cells of *S. elongatus* (*52*, *53*); (ii) differences in the effects of various cations and anions (*54*); and (iii) the absence of the $g = 4.1$ signal in cyanobacteria (*55*). Also, the protein compositions of their PSII complexes are known to be slightly different. For example, the extrinsic 12 kDa and the cytochrome *c*550 regulatory subunits of PSII in cyanobacteria have been replaced in higher plants by proteins with apparent molecular weights of 17 and 23 kDa (*56*). Furthermore, the intrinsic psbW protein is probably absent in cyanobacteria (*6*), and $P680^+Q_A^-$ charge recombination appears to occur ~8 times slower in cyanobacteria than in higher plants (*57*).

Here, we employ FIOPs to compare the temperature dependents of the miss and double hit probabilities and of the S state lifetimes in *S. elongatus* and spinach. This study reveals clear differences on the acceptor side of PSII, which are most likely related to the elevated growth temperature of *S. elongatus*. Furthermore, slight differences in the redox potential of Y_D/Y_D^{ox} have been found.

MATERIALS AND METHODS

Sample Preparation. The thermophilic cyanobacterium *S. elongatus* was grown at 56 °C, and cells were harvested at the mid to late log phase. Thylakoids of *S. elongatus* were isolated from whole cells using a YEDA press (*58*). They were washed several times, frozen as beads in liquid nitrogen ([Chl] = 0.76 mM), and stored at −70 °C until used. Spinach thylakoids were isolated according to standard procedures. After final centrifugation and resuspension to a chlorophyll concentration of [Chl] = 6 mM, they were also frozen as beads in liquid nitrogen and then stored at −70 °C until used. Before the measurements, the thylakoid beads were thawed in the dark on ice and diluted to [Chl] = 0.15 mM (*S. elongatus*) or 0.8 mM (spinach) with MCMH buffer (400 mM mannitol, 20 mM $CaCl_2$, 10 mM $MgCl_2$, and 50 mM HEPES/NaOH at pH 6.8 and 4 °C).

The FIOPs were measured with an unmodulated home-built Joliot-type bare platinum electrode (*59*, *60*), which keeps the temperature of the electrode constant within 0.3 °C. Samples were transferred to the electrode in very dim green light. To ensure complete sedimentation and temperature equilibration, 10 μL aliquots of thylakoids from *S. elongatus* and spinach were kept for 5 and 3 min, respectively, on the electrode at the given temperature. For flash excitation, a xenon flash lamp (EG&G, model PS 302, light pack FY-604) was used that was trigged from a personal computer. Data were recorded with a sampling rate of 3 ms/point, and the flash rate was 2 Hz. No exogenous electron acceptors were added.

For oxygen evolution measurements, two kinds of samples were used: (i) S_1Y_D samples containing a high percentage of the reduced form of tyrosine D, Y_D, because of long-term storage at −70 °C (*60*−*62*) and (ii) $S_1Y_D^{ox}$ samples with Y_D oxidized in about 90% of the centers. In the case of spinach thylakoids, $S_1Y_D^{ox}$ samples were obtained by excitation of S_1Y_D thylakoids with one saturating flash directly on the Joliot type electrode and 5 min of dark adaptation before the FIOPs were recorded. Because of the very slow S_2 state decay in *S. elongatus* thylakoids (see Results), these samples had to be flashed and dark-adapted in glass vials. To ensure oxidation of most Y_D in the *S. elongatus* thylakoids under these conditions, the *S. elongatus* samples were flashed twice in 50 μL aliquots ([Chl] = 0.15 mM) by a frequency doubled Nd:YAG laser (532 nm, 800 mJ/pulse), with an intermediate dark-adaptation of 15 min at room temperature. Afterward, the samples were kept in the dark at room

temperature for 1 h and then stored on ice until the FIOP measurements were performed.

For S_2 and S_3 lifetime measurements, the thylakoids were first sedimented and temperature equilibrated on the Joliot electrode for 3 or 5 min as indicated above. Then, the samples were excited with one or two preflashes, respectively, followed by a flash train of 2 Hz that was started after various dark-adaptation times ranging between 0.5 and 600 s. To observe the $S_0Y_D^{ox} \rightarrow S_1Y_D$ reaction, the sedimented $S_1Y_D^{ox}$ samples were illuminated on the Joliot electrode with three flashes, and after dark-times varying between 1 s and 120 min FIOPs were measured. For all FIOP measurements, the polarization of −750 mV was switched on 40 s before the flash train, and the pH of the flow buffer was adjusted to pH 6.8 at the indicated temperatures. All measurements were repeated at least two times.

Data Analysis. The first 16 flashes of each FIOP were analyzed using an Excel spreadsheet that was based on an extended Kok model, which includes the reduced S_{-1} state and an activity parameter *d* that compensates changes in the number of active PSII centers during the flash train (*44*). This extended Kok model is summarized by eq 1:

$$\begin{bmatrix} S_{-1} \\ S_0 \\ S_1 \\ S_2 \\ S_3 \end{bmatrix}_n = \begin{bmatrix} \alpha & 0 & 0 & 0 & 0 \\ \gamma & \alpha & 0 & \beta & \gamma \\ \beta & \gamma & \alpha & 0 & \beta \\ 0 & \beta & \gamma & \alpha & 0 \\ 0 & 0 & \beta & \gamma & \alpha \end{bmatrix} \begin{bmatrix} S_{-1} \\ S_0 \\ S_1 \\ S_2 \\ S_3 \end{bmatrix}_{n-1} d \qquad (1)$$

where $\gamma = 1 - \alpha - \beta$ is the single hit probability, and *n* is the flash number.

Equation 1 implies the assumption of equal miss and double hit probabilities for all S state transitions. For some fits of Table 2, S state dependent miss or double hit parameters were used under special constraints, which are outlined in the Results:

$$\begin{bmatrix} S_{-1} \\ S_0 \\ S_1 \\ S_2 \\ S_3 \end{bmatrix}_n = \begin{bmatrix} \alpha_{-1} & 0 & 0 & 0 & 0 \\ \gamma_{-1} & \alpha_0 & 0 & \beta_2 & \gamma_3 \\ \beta_{-1} & \gamma_0 & \alpha_1 & 0 & \beta_3 \\ 0 & \beta_0 & \gamma_1 & \alpha_2 & 0 \\ 0 & 0 & \beta_1 & \gamma_2 & \alpha_3 \end{bmatrix} \begin{bmatrix} S_{-1} \\ S_0 \\ S_1 \\ S_2 \\ S_3 \end{bmatrix}_{n-1} d \qquad (2)$$

where, for example, $\gamma_1 = 1 - \alpha_1 - \beta_1$.

The oxygen yield of the *n*th flash, Y^f_n, was calculated using eq 3

$$Y^f_n = (1 - \alpha)[S_3]_{n-1} + \beta[S_2]_{n-1} \qquad (3)$$

for the equal miss case and by eq 4, if S state dependent misses or double hits were considered

$$Y^f_n = (1 - \alpha_3)[S_3]_{n-1} + \beta_2[S_2]_{n-1} \qquad (4)$$

The program is minimizing the expression

$$dy^2_n = \sum_{n=1}^{F} (Y^{exp}_n - Y^f_n \sum_{n=1}^{F} Y^{exp}_n / \sum_{n=1}^{F} Y^f_n)^2 \qquad (5)$$

where Y^{exp}_n is the relative oxygen yield of the *n*th flash, and *F* is the number of analyzed flashes.

Scheme 2: Extended Kok Model that Takes into Account S State Redistributions Resulting from the Fast Reductions of the S_2 and S_3 States by Y_D during a Flash Train[a]

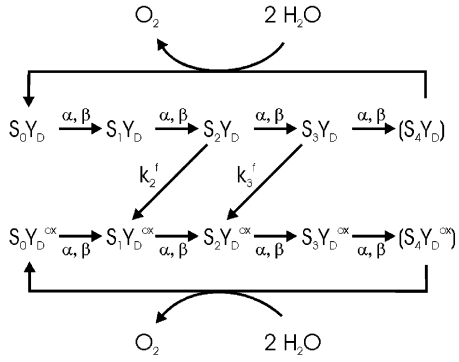

[a] See text for details.

The normalization is given by

$$\sum_{i=-1}^{3} [S_i] = 1 \qquad (6)$$

Effects arising from fast reductions of S_2 and S_3 by Y_D between flashes (e.g., see Figure 1) have been taken into account by further extending the Kok model according to Scheme 2 (see also refs *22* and *63*).

Such corrections are of special relevance for *S. elongatus* thylakoids at high temperatures. The required first-order rate constants (k^f_2, k^f_3) and the percentage of reduced tyrosine in the samples were determined from lifetime measurements in an iterative process that is described below. Only minor corrections for the miss and double hit probabilities resulted from this process for preflashed ($S_1Y_D^{ox}$) samples. In Scheme 2, it is assumed that the miss and double hit probabilities are independent of the redox state of tyrosine D. The validity of this approximation is analyzed in this paper (see Table 2).

The fit quality is calculated according to eq 7:

$$fq = \frac{dy^2_n}{(F - P)} \qquad (7)$$

where *P* is the number of free parameters used.

To cope with effects arising from the fast S_2 and S_3 state reductions by Y_D, the S state lifetime data were analyzed in three cycles. In the first step, the data of the flash train were deconvoluted into S state populations ignoring back reactions of S_2 and S_3 with Y_D and using the miss and double hit probabilities determined from the preflashed samples at the respective temperatures. The semilogarithmic plot of these values versus time was used as a first estimate of the rate constants for fast and slow decay. In the second step, these estimates were used to improve the fits by including Y_D back reactions between flashes, as described above. In the third step, these improved rate constants were used to obtain the final rate constants given in the text and tables. Only very small changes were obtained by applying the third step of fitting.

The rate constants for the fast (k^f_i) and slow (k^s_i) S_2 and S_3 decay were calculated according to eq 8:

$$S_i(t) = A_i e^{-k^f_i t} + B_i e^{-k^s_i t} \qquad (8)$$

where $i = 2$, 3, and t is the dark-time between the last preflash and the first flash of the detecting flash train. A_i and B_i are the relative amplitudes of fast and slow decay, respectively.

For the S_0 oxidation to S_1, a simple one exponential decay was assumed:

$$S_0(t) = S_0(t = 0)e^{-k_0 t} \quad (9)$$

Half-times were calculated according to

$$t_{1/2} = (\ln 2)/k \quad (10)$$

Activation energies were determined from the slope of Arrhenius-type plots (ln k vs T^{-1}).

RESULTS

In this study, we used two types of samples: (i) long time dark-adapted thylakoids with a high percentage of reduced tyrosine D (S_1Y_D samples) and (ii) thylakoids, in which tyrosine D was largely oxidized because of a combination of a preflash treatment and subsequent dark-adaptation ($S_1Y_D^{ox}$ samples, for details see Materials and Methods). Figure 1 shows normalized flash-induced oxygen evolution patterns (FIOPs) measured at 20 °C in *S. elongatus* thylakoids with high populations of states $S_1Y_D^{ox}$ (closed symbols) and S_1Y_D (open symbols). In both cases, the typical period four oscillations are observed with maxima in the third and seventh flashes. However, the $S_1Y_D^{ox}$ sample gives rise to a clearly more pronounced oscillation than the S_1Y_D thylakoids. A detailed analysis (Table 2) within the framework of an extended Kok model, which takes into account partial reductions of redox states S_2 and S_3 by Y_D during the dark-time between the flashes (Scheme 2), showed that the observed differences between these two sample types can be accounted for by (i) a larger extent of reduction of S_2 and S_3 by Y_D during the flash train in the S_1Y_D as compared to the $S_1Y_D^{ox}$ thylakoids; (ii) a somewhat increased S_0 population in S_1Y_D thylakoids; and (iii) a slightly higher miss parameter in S_1Y_D samples. The percentage of reduced tyrosine D used in the fits as fixed parameters was determined from the relative amplitude of fast S_2 state decay, which yielded values of 55 and 11% for S_1Y_D and $S_1Y_D^{ox}$ samples, respectively (see inset of Figure 1).

For the following comparison of the temperature dependencies of the miss and double hit parameters of spinach and *S. elongatus* PSII, we used $S_1Y_D^{ox}$ thylakoids since these samples allow a determination of parameters α and β essentially without interference by the fast back reactions of Y_D with the S_2 and S_3 states. Figure 2 shows three original FIOP traces of *S. elongatus* thylakoids at 3 °C (top), 20 °C (middle), and 40 °C (bottom). In $S_1Y_D^{ox}$ thylakoids, the ratio of the fourth to third flashes (or eighth to seventh flashes and so on) is a suitable qualitative measure for the miss parameter, while the relative amplitude of the second flash is representative for the double hit probability. The FIOPs of *S. elongatus* thylakoids monitored at different amplification factors show that the relative amplitude of the second flash (double hit probability) increases with increasing temperature. In contrast, the ratio of the fourth to third flashes (misses) attains its minimum at 20 °C and increases at lower and higher temperatures. While the double hit probability

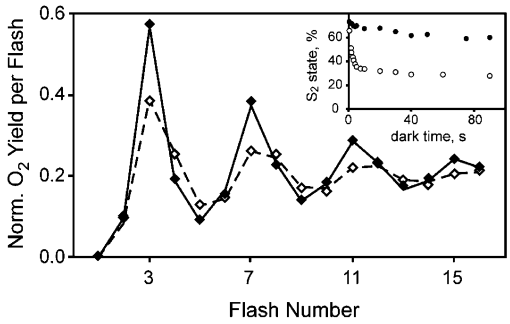

FIGURE 1: Normalized FIOPs of $S_1Y_D^{ox}$ (closed symbols) and S_1Y_D (open symbols) thylakoids of *S. elongatus* at 20 °C and pH 6.8. Lines correspond to fits C and I of Table 2. Inset: $S_2 \rightarrow S_1$ decay of $S_1Y_D^{ox}$ (closed symbols) and S_1Y_D (open symbols) thylakoids of *S. elongatus* under the same conditions.

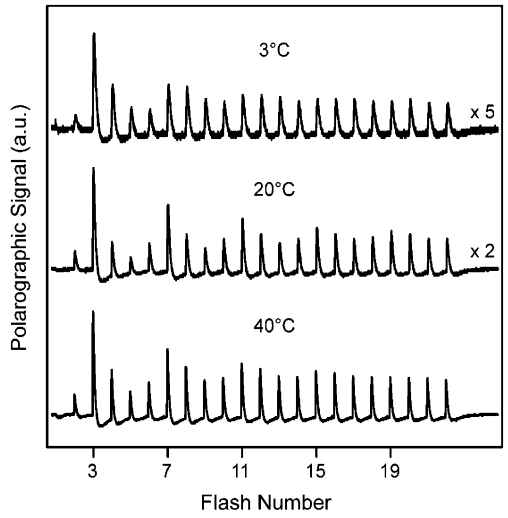

FIGURE 2: Original FIOPs of $S_1Y_D^{ox}$ thylakoids from *S. elongatus* measured at 3, 20, or 40 °C and pH 6.8.

of *S. elongatus* thylakoids follows the trend observed earlier for spinach samples (*23*, *64*), the temperature dependence of the miss parameters appears to differ significantly from the known trend. With spinach thylakoids, it was observed that the ratio of the fourth to third flashes increases continuously with increasing temperature (*23*). To better characterize this difference, we measured FIOPs of spinach and *S. elongatus* thylakoids at various temperatures between 3 and 35 °C and analyzed them with an extended Kok model (eq 1). The obtained values for the miss parameter α and the double hit probability β are depicted in Figure 3 as a function of temperature. For spinach thylakoids, these data agree with those of a previous report, although the absolute value at low temperature is about 2% higher (*23*). In case of *S. elongatus* thylakoids, this quantitative analysis confirms the very different temperature dependence of the miss parameter in this organism and shows that the lowest values for α are obtained at 25 °C under our conditions. A comparison of the α values between the two species shows that at temperatures below 10 °C, a clearly lower probability for misses is found in spinach, while at temperatures between 20 and 35 °C this parameter is lower in *S. elongatus*. Above 35 °C the OEC of spinach starts to lose its functional and structural integrity (*65*), and therefore, a comparison is meaningless. The double hits increase in both spinach and *S. elongatus* almost linearly with temperature, but the β

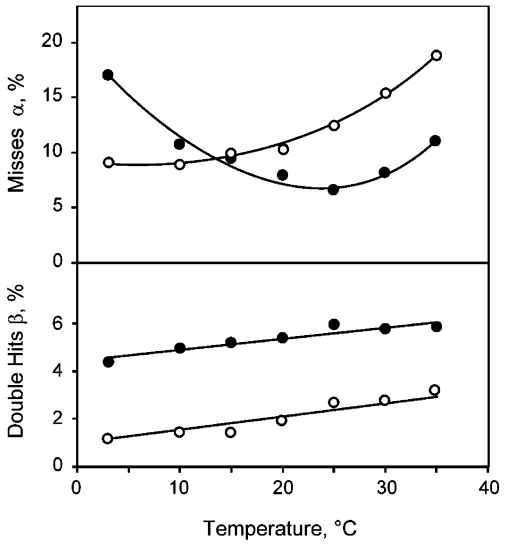

FIGURE 3: Temperature dependence of the miss (top) and double hit (bottom) probabilities of $S_1Y_D^{ox}$ thylakoids from *S. elongatus* (closed symbols) and spinach (open symbols). The pH was adjusted to 6.8 at the given temperatures. S state independent miss (α) and double hit (β) probabilities were calculated from FIOPs using the extended Kok model described in eq 1 and in fit C of Table 2.

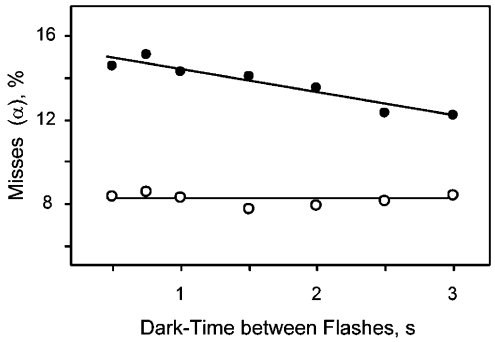

FIGURE 4: Dependence of the miss parameter α on the dark-time between all flashes of a train in $S_1Y_D^{ox}$ thylakoids of *S. elongatus* (closed symbols) and spinach (open symbols). The measurements were recorded at 3 °C and pH 6.8. The S state independent miss parameters were calculated from FIOPs using the extended Kok model described in eq 1 and in fit C of Table 2.

values are generally higher in *S. elongatus* by an increment $\Delta\beta$ of about 3%.

The high miss parameter at low temperatures in *S. elongatus* could be either caused by temperature-dependent shifts of redox equilibria between PSII cofactors or by a kinetic limitation. To address this problem, we varied at a measuring temperature of 3 °C the dark-times between all flashes of the illuminating flash train between 500 ms (2 Hz) and 3 s (0.33 Hz). As expected for these conditions (Figure 4), essentially no change is observed for a miss parameter with spinach samples. In contrast, a clear decline of the miss parameter from 15% at $t_d = 500$ ms down to about 12% at $t_d = 3$ s is observed for *S. elongatus* thylakoids. These data support the idea that a rate-limiting step contributes in *S. elongatus* to the increase of the miss parameter at temperatures below 15 °C.

A further characteristic property of the OEC is the lifetime of the S states. Figure 5 shows a semilogarithmic plot of the S_2 and S_3 decay at 20 °C in $S_1Y_D^{ox}$ thylakoids. Since in these samples most tyrosine D was oxidized by a preflash treatment, the S_2 and S_3 decay is dominated by the slow phase

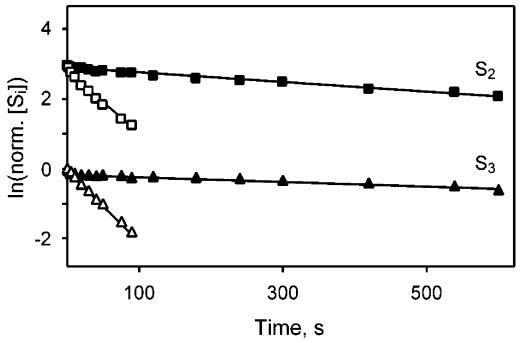

FIGURE 5: Semilogarithmic plot of the S_2 (squares) and S_3 (triangles) state decay in Y_D^{ox} thylakoids from *S. elongatus* (closed symbols) and spinach (open symbols). The lifetime measurements were performed at 20 °C and pH 6.8. For details of data deconvolution see Materials and Methods.

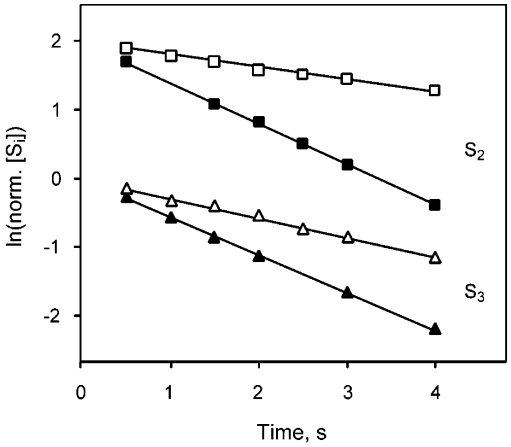

FIGURE 6: Semilogarithmic plot of the fast phase of S_2 (squares) and S_3 (triangles) state decay in Y_D thylakoids from *S. elongatus* (closed symbols) and spinach (open symbols). The lifetime measurements were performed at 20 °C and pH 6.8. For details of data deconvolution see Materials and Methods. The pure fast phase was isolated through subtraction of the slow component from the original data.

of reduction. On the basis of thermoluminescence experiments, the dominant donor for this slow reaction should be Q_B^- (*18*, *53*), but Q_BH_2 or even other electron donors may contribute as well. The data of Figure 5 reveal that the slow relaxations of S_2 and S_3 are 15 and 30 times slower, respectively, in *S. elongatus* than in spinach. This is in qualitative agreement with earlier data gathered from measurements of thermoluminescence and FIOPs in whole cells of *S. vulcanus* (*52*), where retardations by factors of 4 and 7 were observed.

It seems unlikely that the differences in the slow relaxation rates between *S. elongatus* and spinach thylakoids are due to changes of distance between Q_B and the Mn_4O_xCa complex (or between other intermediate cofactors) in the two species. Therefore, the results of Figure 5 raise questions about redox-potential shifts either on the donor and/or the acceptor side of PSII (see also ref *53*). In the case of donor side effects, the rates of the fast S_2 and S_3 reductions by Y_D are expected to change in a similar way as the slow relaxation rates. This was tested using S_1Y_D thylakoids, and the results are displayed in Figure 6. It is obvious that for these reactions the differences are much less pronounced than for the slow phase of S_2 and S_3 decay. Remarkably, in this case the S_2 and S_3 states are more stable by a factor of 2 to 3 in spinach

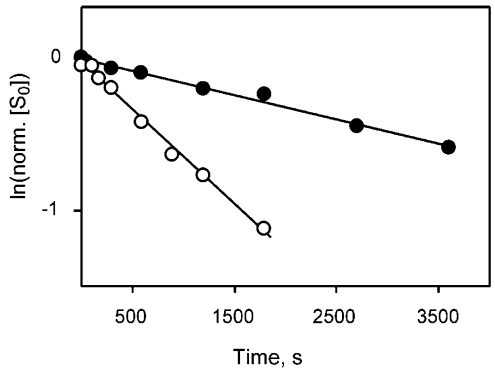

FIGURE 7: Semilogarithmic plot of the S_0 state population as a function of dark-adaptation time at 20 °C and pH 6.8. The measurements were performed with Y_D^{ox} thylakoids from *S. elongatus* (closed symbols) and spinach (open symbols). For details of data deconvolution see Materials and Methods.

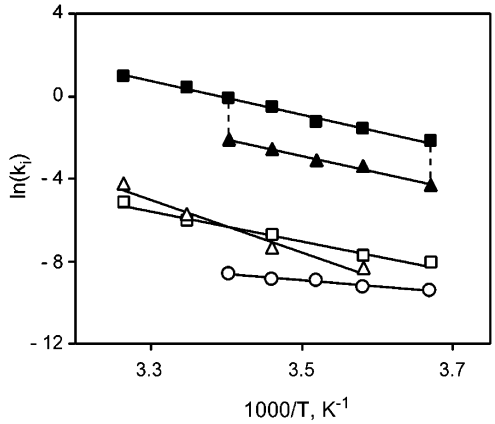

FIGURE 8: Arrhenius-type plot of the rate constants of the S_2 (squares), S_3 (triangles), and S_0 (circles) decay in *S. elongatus* thylakoids. Closed symbols, fast S_2 and S_3 decay through reduction by Y_D; open squares and triangles, slow S_2 and S_3 decay by other electron donors (e.g., Q_B^-); and circles, S_0 oxidation to S_1 by Y_D^{ox}. For the sake of clarity, the data for the fast S_3 decay are displaced by a constant downshift indicated by broken lines. The obtained activation energies are presented in Table 1.

than in *S. elongatus* thylakoids. On the basis of these findings, it seems unlikely that donor side effects are the dominating factor for the large differences shown in Figure 5. In line with the S_2 and S_3 reduction by Y_D also, the oxidation of S_0 to S_1 by Y_D^{ox} proceeds at 20 °C with a rate that differs only slightly from that of the spinach samples. However, in contrast to the fast S_2 and S_3 reductions by Y_D, the S_0 oxidation by Y_D^{ox} is 4 times slower in *S. elongatus* than in spinach as illustrated in Figure 7.

The comparative lifetime measurements presented in Figures 5−7 reflect the properties of the S states at 20 °C. Since the relaxations of S_2 and S_3 were shown to be reactions with comparatively high activation energies in spinach samples (*22*, *23*, *64*), some of the observed differences might originate from the species dependent characteristics of thermal activation. Therefore, S state lifetime measurements at various temperatures between 3 and 35 °C were performed. Figure 8 shows the results for the fast and slow S_2 and S_3 decay and the S_0 oxidation to S_1 in *S. elongatus* thylakoids. The activation energies calculated from these data are compiled in Table 1, which for comparison also presents previously reported values for spinach samples. An inspection of these values reveals that for a given S state all activation

Table 1: Comparison of Activation Energies for S State Decay in *S. elongatus* and Spinach

	S. elongatus	spinach		
	thylakoids pH 6.8 (kJ mol^{-1})	BBY pH 6.5 (kJ mol^{-1})	thylakoids pH 7.0 (kJ mol^{-1})	thylakoids pH 7.5 (kJ mol^{-1})
S_2 fast	68 ± 3	60 ± 10	55	47
S_3 fast	69 ± 3	55 ± 10	50	44
S_2 slow	60 ± 3	80 ± 5	85	63
S_3 slow	106 ± 6	75 ± 5	75	73
S_0	28 ± 3		30	
ref	this paper	*64*	*23*	*22*

energies of *S. elongatus* are within a factor of 1.5 from those previously reported for spinach (*22*, *23*, *64*). Interestingly, the differences between the slow S_2 and S_3 decay is larger in *S. elongatus* (factor of 1.8) than in spinach (factor of 0.9−1.2).

On the basis of the obtained rate constants for the fast S_2 and S_3 decay, detailed analyses of the FIOPs of S_1Y_D and $S_1Y_D^{ox}$ thylakoids were performed to address two relevant problems: (a) the validity of the approximation of S state independent probabilities of misses and double hits and (b) possible effects of the redox state of Y_D on the energetics of $P680^{+\bullet}$.

The values in rows A−F in Table 2 are the results of a systematic fit approach for the $S_1Y_D^{ox}$ sample. In fit A, we start with the assumption of 100% S_1 state population and only the two S state independent parameters α and β were free running. The damping parameter *d*, which accounts for possible changes of the number of active PSII centers during the flash train, was found to be within the range of $0.99 \leq d \leq 1.00$ for all fits of this study and is therefore not shown in Table 2. Fit A also accounts for the fast relaxation reactions of S_2 and S_3 by using the above determined values of Y_D population and the rate constants of the fast S_2 and S_3 decay measured at 20 °C ($Y_D = 11\%$, $k_3^f = 0.54$ s^{-1}, $k_2^f = 0.60$ s^{-1}).

With this procedure, a good overall description of the data could be achieved. However, a closer inspection revealed some small systematic deviations after the fifth and following flashes. As expected from this feature, the inclusion of S_2 and S_0 as free parameters (fit B) gives rise to a fit of only a slightly (10%) higher quality. However, if also the redox state S_{-1} is included as a free running parameter, a drastic improvement by a factor of 3 (fit C) is obtained, and the data are almost perfectly simulated as illustrated in Figure 1, where fit C is shown as a solid line. Fit D shows that setting Y_D to zero has only a minor effect on the deconvolution of the FIOP of this preflashed sample (the α and S_0 parameters are only slightly larger).

The above fit result that suggests the existence of S_{-1} in the preflashed $S_1Y_D^{ox}$ is not easily understandable and requires additional assumptions (e.g., small S_{-2} population or fast reduction in a small fraction of PSII) that are difficult to rationalize. However, we consistently find also for spinach samples an improvement of fit quality for dark-adapted samples if a small percentage of S_{-1} is included in the fits of FIOPs (*44*). In this respect, it is very important to note that a quite similar apparent S_{-1} population (and no S_{-2} population) is required for the best fit of the FIOP of the nonpreflashed sample (fit H). Therefore, it seems more likely

Table 2: Fits of the Flash Induced Oxygen Evolution Patterns (FIOPs) of Long-Term Dark-Adapted S_1Y_D Thylakoids and of Preflashed $S_1Y_D^{ox}$ Thylakoids from *S. elongatus*[a]

		fit parameters (%)									goodness of fit	
sample	fit	α	α_2	α_3	β	S_2	S_1	S_0	S_{-1}	Y_D	dx^2 ($\times 10^{-6}$)	fq ($\times 10^{-6}$)
$S_1Y_D^{ox}$	A	9.5			6.4		100*			11*	115	8.9
	B	8.5			6.2	1.2	92.6	6.2		11*	80	8.0
	C	8.1			5.4	2.1	87.9	3.8	6.2	11*	25	2.8
	D	8.6			5.4	2.5	85.3	6.2	6.3		24	2.7
	E		15.8	15.8	5.9		100*			11*	55	4.3
	F		30.0		5.2		100*			11*	21	1.6
S_1Y_D	G	13.2			7.7		100*			55*	217	16.7
	H	8.4			5.8	5.6	72.5	15.5	6.4	55*	5	0.6
	I	9.0			7.6		79.0	17.1	3.9	55*	51	5.1
	J	12.5			7.4		68.4	27.8	3.8		110	11.0
	K		17.5	17.5	7.2		87.9	12.1		55*	45	4.1
	L		30.3		6.4		84.0	16.0		55*	52	4.7

[a] The FIOPs of S_1Y_D and $S_1Y_D^{ox}$ obtained at 20 °C and pH 6.8 (open and closed symbols in Figure 1, respectively) were fit using different approaches, which are outlined in the text. For fits A−D and G−J, a Kok model with S state independent miss and double hit parameters was used. In fits E and K, the miss parameters of the $S_2 \rightarrow S_3$ and $S_3 \rightarrow S_0$ transitions (α_2 and α_3, respectively) were forced to be equal, while those for the $S_0 \rightarrow S_1$ and $S_1 \rightarrow S_2$ transitions (α_0 and α_1, respectively) were fixed to 0. In Fits F and L, only α_2 was varied freely, while those of the other S state transitions were fixed to 0. If no values are given for a parameter, it was excluded from the fit. Asterisks indicate that the parameter was fixed to the specified value. The values of 11 and 55% Y_D population for the $S_1Y_D^{ox}$ and S_1Y_D samples, respectively, and the rate constants for the fast S_3 and S_2 decay ($k_3^f = 0.54\ s^{-1}$, $k_2^f = 0.60\ s^{-1}$) were obtained from S_2 and S_3 state lifetime measurements (see Figures 1, 5, and 6). The goodness of fit parameter was calculated as outlined in Materials and Methods.

that the apparent S_{-1} population is a parameter that simply compensates for imperfections of the Kok model used to describe the data. One important approximation of the applied Kok scheme is the assumption of equal misses for each S state transition (see introductory paragraphs). To check whether this approximation can possibly account for the described differences between normal fits and the data, fits were performed assuming various unequal miss models (eq 2). With S state dependent misses no unique solution can be found (*66*), and only two special cases shall be discussed below (fits E and F).

On the basis of recent studies on a correlation between the extent of microsecond components in the $P680^{+\bullet}$ reduction kinetics and the α values (*67*, *38*) and taking into account the period four oscillation of these reactions (*68*, *69*), the miss probabilities for oxidation of S_0 and S_1 are assumed to be small as compared with those of the oxidation of S_2 and S_3. Therefore, we assumed for simplicity in fit E that the miss parameters for the $S_0 \rightarrow S_1$ and $S_1 \rightarrow S_2$ transitions (α_0 and α_1, respectively) are zero, and those of the $S_2 \rightarrow S_3$ and $S_3 \rightarrow S_0$ transitions (α_2 and α_3) are identical. Application of this simple model of S state dependent misses gives a fit quality that is twice as good as that of fit A, which assumes identical misses for all S state transitions. Even better fits are obtained when only one miss parameter is varied and the three others are set to zero. This is shown for α_2 in Table 2 (fit F), but very similar results are obtained for α_1 and α_3. In contrast, no reasonable fits are possible if only α_0 is varied (data not shown). It is remarkable that the fit quality of fit F is of similar quality (or even better) as that of fit C without the need to include any S_2, S_0, or S_{-1} population as fit parameters. In this context, it should be noted that similar S state dependent miss fits of S_2 EPR multiline oscillation patterns such as that published in ref *70* show that more than half of the misses have to occur in the $S_1 \rightarrow S_2$ and $S_2 \rightarrow S_3$ transitions (fits not shown), which is at slight variance to the conclusions in ref *38*, where the S_3 oxidation was inferred to account for more than 50% of the misses.

The rate constants of the $S_2 \rightarrow S_3$ and $S_3 \rightarrow S_0$ transitions are similar or even smaller than that of the electron transfer from Q_A^- to Q_B. It is, therefore, reasonable to assume that in these transitions no double hits occur (*16*). In addition, a period two oscillation for the double hits might be expected, which reflects the redox state of Q_B (*71*). Therefore, also the effect of S state dependent double hit parameters on the fits of FIOPs was tested using various models. However, in no tested case was this kind of extension able to account for the 5th flash deviation discussed above (fits not shown). These results show that the assumption of unequal misses is one possible way for a better description of the obtained FIOPs. However, the present data neither provide an unambiguous proof for S state dependent misses nor permit an identification of the S state transition with the highest miss factor.

In the following, we analyze whether the redox state of Y_D affects the miss parameter. The rationale for this analysis is provided by recent reports that the redox potential of P680 may be modulated by the redox state of Y_D (*15*, *72*, *73*). A change of $E_m(P680/P680^{+\bullet})$ should affect its reduction kinetics and may thereby also change the value of α (*38*, *74*). In addition, the redox state of Y_D could change the miss parameter via more indirect effects, for example, through changes in the H-bonding network. Therefore, FIOPs measured in *S. elongatus* thylakoids either preflashed ($S_1Y_D^{ox}$) or extensively dark-adapted (S_1Y_D) were analyzed. Since the rate constants for the reactions of Y_D with S_2 and S_3 and the percentage of reduced tyrosine D were determined by independent measurements, we can use the extended Kok model described in Scheme 2 to separate increases in the apparent value of α, which are caused by fast back reactions of Y_D with S_2 and S_3, from possible effects on the real miss parameter. For the sake of simplicity, the parameters α and β were initially assumed to be independent of the S state (fits G−J). Fit H in Table 2 shows that an excellent fit quality is obtained for S_1Y_D thylakoids by using the Y_D level of 55% gathered from the S_2 lifetime experiments. In this fit, miss and double

hit probabilities are only slightly higher than for the preflashed sample (fit C). An increase of the percentage of Y_D to about 60% leads to an identical miss parameter as in fit C (data not shown). At first glance, these fits seem to indicate that Y_D has a vanishingly small (if any) effect on the miss parameter. However, a closer inspection of the resulting S state populations reveals that about 6% of S_2 state population is required to obtain the excellent fit quality of fit H. This result is puzzling because this value is 2−3 times higher than that obtained from fits of the preflashed sample (see B−D). Furthermore, it should be expected that the S_2 population in the extremely long-term dark-adapted S_1Y_D samples is zero and in any case cannot exceed the level of the preflashed sample. Therefore, in fit I we have fixed the S_2 population to zero. Under this constrain, miss and double hit probabilities are calculated for the S_1Y_D sample, which are significantly higher than for the $S_1Y_D^{ox}$ sample (fit C). Taking into account that the S_1Y_D sample contains only about 55% Y_D, the result of fit I suggest that for a sample where all PSII complexes have tyrosine D in its reduced form, the miss parameter might be higher by an increment of about 2% as compared to a sample where all tyrosine D is oxidized. To test whether this result is specific for the extended Kok model used in fits C and I, the S_1Y_D data were also analyzed using the 100% S_1 state approach of fit A (see fit G) and by excluding the fast back reactions of Y_D (compare fit J with fit D). Also, in these two cases a significantly higher miss parameter was found for the S_1Y_D sample than for the $S_1Y_D^{ox}$ sample. Similarly, using the $\alpha_2 = \alpha_3$ unequal miss approach in fit K results in a clearly higher miss for the S_1Y_D sample (as compared to fit E). One exception appears to be fit L, where only α_2 was varied. In this case, the miss parameter is almost identical to that of fit F. However, for this fit only a shallow minimum exists, where the values of the miss parameter and the S_0 population are highly dependent on each other. Constraining the S_0 population, for example, to 12% as seen in fit K results in α_2 of about 32% without a significant effect on the fit quality (data not shown).

DISCUSSION

The present study compares in detail the period four oscillations of FIOPs of dark-adapted thylakoids from thermophilic cyanobacteria (*S. elongatus*) and higher plants (spinach). The aim was to address the following three problems concerning the mechanism of water oxidation in PSII: (a) Do evolutionary changes exist at the level of the water oxidation between thermophilic cyanobacteria and higher plants? (b) Is the miss parameter α dependent on the S state? (c) Does the redox state of Y_D affect the miss parameter through mechanisms other than the fast back reactions with S_2 and S_3?

Differences between PSII from Spinach and S. elongatus. In this paper, several functional differences between PSII from spinach and *S. elongatus* have been described: (i) double hits are generally higher in *S. elongatus* than in spinach thylakoids; (ii) at 20 °C, the slow reduction of S_2 and S_3 by electron donors other than Q_A^- and Y_D is more than 1 order of magnitude slower in *S. elongatus*; (iii) in contrast, the reduction of S_2 and S_3 by Y_D is 2−3 times faster in *S. elongatus*, whereas the rate of S_0 oxidation by Y_D^{ox} is 4 times slower; and (iv) the temperature dependence of the miss parameter is strikingly different in *S. elongatus* as compared to that known for spinach, with a surprisingly high value at temperatures close to 0 °C.

The generally higher double hit parameter is a clear indication for a faster electron transfer from Q_A^- to Q_B (Q_B^-) in *S. elongatus* since at least for the S_0 and S_1 states the rate of Q_A^- reoxidation by Q_B (Q_B^-) is the rate-limiting step for a second stable turnover of PSII, which can be caused by the residual light intensity (tail) of microsecond xenon flashes (*16*, *35*). In a former study, the double hit probability was inferred to be almost linearly related to the rate constant of the Q_A^- reoxidation (see Appendix of ref *23*). On the basis of this approximation, the data of this study suggest that the reoxidation of Q_A^- is 2−4 times faster in *S. elongatus* than in spinach thylakoids. This reaction depends also on the conformational flexibility of the protein matrix (*75*, *76*). Accordingly, the difference in the kinetics between both sample types could be explained (i) by changes in redox potentials of Q_A or Q_B; (ii) a slightly shorter distance between Q_A^- and Q_B (Q_B^-); or (iii) by faster protein dynamics in *S. elongatus*. This phenomenon has to be clarified in further detailed investigations that are beyond the scope of the present study.

An independent line of evidence in support of the idea that the acceptor sides of *S. elongatus* and spinach are different is the significant retardation of the slow S_2 and S_3 decay in *S. elongatus* in marked contrast to the much smaller change in the opposite direction of the fast reduction by Y_D. The most straightforward interpretation is that in *S. elongatus* the reduced forms of Q_B are better stabilized than in spinach. This interpretation is in line with thermoluminescence measurements on intact *S. elongatus* cells, in which a stabilization of states $S_2Q_B^-$ and $S_3Q_B^-$ was found (*52*). However, a similar increase in lifetime and temperature was also seen for the thermoluminescence bands of the states $S_2Q_A^-$ and $S_3Q_A^-$. Therefore, on the basis of these thermoluminescence experiments it was not possible to separate donor and acceptor side effects. At temperatures close to 0 °C, the proposed stabilization of reduced plastoquinone in its pocket at the acceptor side might imply a slow exchange of plastoquinol by plastoquinone from the pool in the thylakoid membrane. The different lipid composition of the thylakoid membranes of the thermophilic *S. elongatus* and mesophilic spinach may contribute to this effect. A slow quinol/quinone exchange would explain the high miss parameter at low temperatures in *S. elongatus* and its frequency dependency.

The recent finding of an about eight times slower $P680^+Q_A^-$ recombination in cyanobacteria as compared to higher plants (*57*) may also point to a stabilization of the acceptor side redox intermediates in cyanobacteria. Because the S_2 and S_3 reduction by Q_B^- probably involves Q_A and P680 as intermediates, it is possible that the slower $P680^+Q_A^-$ recombination rate contributes to the effects described in this study. However, this effect is unlikely to be a dominating factor because (i) the retardation of $P680^+Q_A^-$ recombination is significantly smaller than that observed for the slow phases of S state decay and (ii) it also appears to apply to mesophilic cyanobacteria (*57*).

When considering a possible physiological role for drastic retardation of the rates of the slow S_2 and S_3 decay of *S. elongatus* at 20 °C, it is interesting to extrapolate the data to the growth temperature of these cyanobacteria by using

the activation energies gathered from the Arrhenius plot (Figure 8). It turns out that at 55 °C the rates for the slow S_2 and S_3 decay are only slightly faster in *S. elongatus* than those measured for spinach at 20 °C. Therefore, it appears that the acceptor side of *S. elongatus* PSII has been modified in a way that prevents too fast S_2 and S_3 recombinations with electrons from the acceptor side at its growth temperature. Such fast recombinations would significantly reduce the efficiency of oxygen evolution, especially under low light conditions (see also ref *53*).

Differences between *S. elongatus* and spinach thylakoids on the donor side of PSII are less significant as reflected by comparatively small factors of 2−3 for the fast rates of S_2 and S_3 reduction by Y_D and of about 4 for the oxidation of S_0 by Y_D^{ox}. The opposite trend of both reactions could be explained by a minor change in the redox potential of the Y_D/Y_D^{ox} couple. Changes of the redox potential of the S states of the Mn_4O_xCa complex itself are less likely because of the similarities in the EPR and EXAFS properties (see introductory paragraphs). Likewise, former studies clearly showed that the activation energies of the stepwise oxidation of the OEC are very similar in the thermophilic cyanobacterium *S. vulcanus* (*46*) and PSII membrane fragments from spinach (*47*). In summary, this study demonstrates for the first time that the stabilization of the $S_2Q_B^-$ and $S_3Q_B^-$ states in thermophilic cyanobacteria as compared to spinach is predominantly caused by changes in the redox potentials of the acceptor side quinones rather than the S states.

Effect of Tyrosine D on the Miss Parameter. The detailed FIOP measurements and their analyses within the framework of an extended Kok model that takes the fast $S_2Y_D \rightarrow S_1Y_D^{ox}$ and $S_3Y_D \rightarrow S_2Y_D^{ox}$ reactions into account were used to address the question of a possible direct effect of the redox state of Y_D on the miss parameter. It has been suggested that the positive charge in the form of a proton trapped in the microenvironment of Y_D^{ox} enhances the midpoint potential of P680/$P680^{+\bullet}$ via electrostatic interactions (*15*, *72*, *73*). This effect could reduce the extent of microsecond kinetics in the multiphasic pattern of $P680^{+\bullet}$ reduction by Y_Z thus giving rise to a decrease of the probability of misses (*74*). On the basis of the reasonable assumption that in S_1Y_D samples the S_2 population is practically zero because of the very long dark-storage required for their generation, our detailed analyses of FIOPs show that the probabilities of misses is somewhat smaller in $S_1Y_D^{ox}$ samples than in S_1Y_D samples. This suggests that the positive charge in the vicinity of Y_D^{ox} affects the redox equilibria and/or electron-transfer kinetics between PSII cofactors. However, the precise mechanism for this effect cannot be deduced from FIOP measurements, and for most practical applications this effect is small enough to be ignored. One consistent explanation for this fit result is the above-discussed concept of an E_m(P680/$P680^{+\bullet}$) modulation by Y_D^{ox}. Another possible explanation may be provided by a recent publication on PSII complexes from *Chlamydomonas* mutants. These authors concluded that the substitution of Y_D by phenylalanine affects the hydrogen bond network, which regulates the microsecond kinetics of $P680^{+\bullet}$ reduction (*77*). It therefore appears also possible that Y_D^{ox} affects the miss parameter via changing the H-bonding network within PSII.

Unequal Misses. The detailed fits of Table 2 show that Kok models assuming S state independent miss and double hit parameters lead to a small, systematic under-estimation of the oxygen yield in the 5th flash of FIOPs of dark-adapted thylakoids. This problem can be numerically solved by either including the S_{-1} state in the fits or alternatively by the assumption of S state dependent misses. If only the fit quality is considered, the data of this study neither permit a distinction between these two options nor exclude further possibilities. However, the finding that preflashing hardly effects the apparent S_{-1} population appears to be a strong argument against a real S_{-1} population in these dark-adapted samples and favor the idea of S state dependent misses, which have already been discussed in previous reports (*16*, *36*, *38*, *78*).

Our fits to the FIOPs only exclude the option that most of the misses occur on the $S_0 \rightarrow S_1$ transition but do not allow a further distinction between other tested options. Therefore, we need to refer to independent data for a further analysis. The known fact that under optimized conditions about the same S_2 EPR multiline signal amplitude can be generated with a single flash excitation of a PSII sample as by continuous illumination at 200 K argues for a fairly small miss parameter for the $S_1 \rightarrow S_2$ transition. On the other hand, our above-mentioned S state dependent miss fits to S_2 EPR multiline patterns reveal that at least half of the misses have to occur during the $S_1 \rightarrow S_2$ and $S_2 \rightarrow S_3$ transitions because otherwise the S_2 multiline amplitude after the 2nd flash cannot be fit with reasonable assumptions. Therefore, the above data indicate that $\alpha_2 \geq \alpha_1 \geq \alpha_0$ and $\alpha_1 + \alpha_2 \geq \alpha_3 + \alpha_0$.

Earlier reports have indeed suggested a high α_2 (*36*, *78*) on the basis of the finding that it is very difficult to achieve light saturation for this transition, while a large α_3 was proposed based on the high extent of a microsecond component for $P680^{+\bullet}$ reduction for this transition (*38*). Therefore, at present it appears to be possible that the $S_2 \rightarrow S_3$ and the $S_3 \rightarrow S_0$ transitions are coupled to higher miss parameters than the other two transitions. However, further studies simultaneously following markers for several S states in one set of samples are required to solve this fundamental question of the Kok cycle. Only with precise numbers at hand will it then be possible to assess possible impacts of S state dependent misses and double hits on the interpretation of many data concerning the kinetics and redox states within the OEC.

ACKNOWLEDGMENT

The authors are thankful to Dr. Athina Zouni and Dörte DiFiore for kindly providing thylakoids of *S. elongatus*.

REFERENCES

1. Britt, R. D. (1996) in *Oxygenic Photosynthesis: The Light Reactions* (Ort, D. R., and Yocum, C. F., Eds.) pp 137−164, Kluwer Academic Publishers, Dordrecht.
2. Nugent, J. H. A. (1996) *Eur. J. Biochem. 237*, 519−531.
3. Yachandra, V. K., Sauer, K., and Klein, M. P. (1996) *Chem. Rev. 96*, 2927−2950.
4. Messinger, J. (2000) *Biochim. Biophys. Acta 1459*, 481−488.
5. Renger, G. (2001) *Biochim. Biophys. Acta 1503*, 210−228.
6. Hankamer, B., Morris, E., Nield, J., Carne, A., and Barber, J. (2001) *FEBS Lett. 504*, 142−151.
7. Zouni, A., Witt, H. T., Kern, J., Fromme, P., Krauss, N., Saenger, W., and Orth, P. (2001) *Nature 409*, 739−743.
8. Kamiya, N., and Shen, J.-R. (2003) *Proc. Natl. Acad. Sci. U.S.A. 100*, 98−103.

9. Yocum, C. F. (1991) *Biochim. Biophys. Acta 1059*, 1−15.
10. Lindberg, K., and Andréasson, L.-E. (1996) *Biochemistry 35*, 14259−14267.
11. Wincencjusz, H., Yocum, C. F., and van Gorkom, H. J. (1998) *Biochemistry 37*, 8595−8604.
12. van Rensen, J. J. S., Xu, C., and Govindjee (1999) *Physiol. Plant. 105*, 585−592.
13. Klimov, V. V., and Baranov, S. V. (2001) *Biochim. Biophys. Acta 1503*, 187−196.
14. Olesen, K., and Andréasson, L.-E. (2003) *Biochemistry 42*, 2025−2035.
15. Diner, B. A., and Rappaport, F. (2002) *Annu. Rev. Plant Biol. 53*, 551−580.
16. Kok, B., Forbush, B., and McGloin, M. (1970) *Photochem. Photobiol. 11*, 457−476.
17. Robinson, H. H., and Crofts, A. R. (1983) *FEBS Lett. 153*, 221−226.
18. Rutherford, A. W., and Inoue, Y. (1984) *FEBS Lett. 165*, 163−170.
19. Vermaas, W. E. J., Renger, G., and Dohnt, G. (1984) *Biochim. Biophys. Acta 764*, 194−202.
20. Styring, S., and Rutherford, A. W. (1987) *Biochemistry 26*, 2401−2405.
21. Rutherford, A. W., Crofts, A. R., and Inoue, Y. (1982) *Biochim. Biophys. Acta 682*, 457−465.
22. Vass, I., Deak, Z., and Hideg, E. (1990) *Biochim. Biophys. Acta 1017*, 63−69.
23. Messinger, J., Schröder, W. P., and Renger, G. (1993) *Biochemistry 32*, 7658−7668.
24. Dismukes, G. C., and Siderer, Y. (1981) *Proc. Natl. Acad. Sci. U.S.A. 78*, 274−278.
25. Casey, J. L., and Sauer, K. (1984) *Biochim. Biophys. Acta 767*, 21−28.
26. Zimmermann, J. L., and Rutherford, A. W. (1984) *Biochim. Biophys. Acta 767*, 160−167.
27. Åhrling, K. A., Peterson, S., and Styring, S. (1997) *Biochemistry 36*, 13148−13152.
28. Messinger, J., Nugent, J. H. A., and Evans, M. C. W. (1997) *Biochemistry 36*, 11055−11060.
29. Messinger, J., Robblee, J. H., Yu, W. O., Sauer, K., Yachandra, V. K., and Klein, M. P. (1997) *J. Am. Chem. Soc. 119*, 11349−11350.
30. Dexheimer, S. L., and Klein, M. P. (1992) *J. Am. Chem. Soc. 114*, 2821−2826.
31. Yamauchi, T., Mino, H., Matsukawa, T., Kawamori, A., and Ono, T.-a. (1997) *Biochemistry 36*, 7520−7526.
32. Campbell, K. A., Peloquin, J. M., Pham, D. P., Debus, R. J., and Britt, R. D. (1998) *J. Am. Chem. Soc. 120*, 447−448.
33. Matsukawa, T., Mino, H., Yoneda, D., and Kawamori, A. (1999) *Biochemistry 38*, 4072−4077.
34. Ioannidis, N., and Petrouleas, V. (2000) *Biochemistry 39*, 5246−5254.
35. Jursinic, P. (1981) *Biochim. Biophys. Acta 635*, 38−52.
36. Renger, G., and Hanssum, B. (1988) *Photosynth. Res. 16*, 243−259.
37. Shinkarev, V., and Wraight, C. A. (1993) *Proc. Natl. Acad. Sci. U.S.A. 90*, 1834−1838.
38. de Wijn, R., and van Gorkom, H. J. (2002) *Photosynth. Res. 72*, 217−222.
39. Debus, R. J. (1992) *Biochim. Biophys. Acta 1102*, 269−352.
40. Renger, G. (1997) *Physiol. Plant. 100*, 828−841.
41. Ono, T.-a. (2001) *Biochim. Biophys. Acta 1503*, 40−51.
42. Tamura, N., and Cheniae, G. (1987) *Biochim. Biophys. Acta 890*, 179−194.
43. Ananyev, G. M., Zaltsman, L., Vasko, C., and Dismukes, G. C. (2001) *Biochim. Biophys. Acta 1503*, 52−68.
44. Messinger, J., Seaton, G., Wydrzynski, T., Wacker, U., and Renger, G. (1997) *Biochemistry 36*, 6862−6873.
45. Messinger, J., Robblee, J., Bergmann, U., Fernandez, C., Glatzel, P., Isgandarova, S., Hanssum, B., Renger, G., Cramer, S., Sauer, K., and Yachandra, V. (2001) in *Proceedings of the 12th International Congress on Photosynthesis*, pp S10−019, CSIRO Publishing, Collingwood, Australia.
46. Koike, H., Hanssum, B., Inoue, Y., and Renger, G. (1987) *Biochim. Biophys. Acta 893*, 524−533.
47. Renger, G., and Hanssum, B. (1992) *FEBS Lett. 299*, 28−32.
48. McDermott, A. E., Yachandra, V. K., Guiles, R. D., Cole, J. L., Dexheimer, S. L., Britt, R. D., Sauer, K., and Klein, M. P. (1988) *Biochemistry 27*, 4021−4031.
49. Boussac, A., Kuhl, H., Ghibaudi, E., Rögner, M., and Rutherford, A. W. (1999) *Biochemistry 38*, 11942−11948.
50. Boussac, A., Sugiura, M., Inoue, Y., and Rutherford, A. W. (2000) *Biochemistry 39*, 13788−13799.
51. Sarrou, J., Isgandarova, S., Kern, J., Zouni, A., Renger, G., Lubitz, W., and Messinger, J. (2003) *Biochemistry 42*, 1016−1023.
52. Govindjee, Koike, H., and Inoue, Y. (1985) *Photochem. Photobiol. 42*, 579−585.
53. Vass, I., and Inoue, Y. (1992) in *The Photosystems: Structure, Function and Molecular Biology* (Barber, J., Ed.) pp 259−294, Elsevier Science Publishers, Amsterdam.
54. Pauly, S., Schlodder, E., and Witt, H. T. (1992) *Biochim. Biophys. Acta 1099*, 203−210.
55. Boussac, A., Kuhl, H., Un, S., Rögner, M., and Rutherford, A. W. (1998) *Biochemistry 37*, 8995−9000.
56. Shen, J.-R., Ikeuchi, M., and Inoue, Y. (1992) *FEBS Lett. 301*, 145−149.
57. de Wijn, R., and van Gorkom, H. J. (2002) *Biochim. Biophys. Acta 1553*, 302−308.
58. Schatz, G. H., and Witt, H. T. (1984) *Photobiochem. Photobiophys. 7*, 1−14.
59. Joliot, P. (1972) *Methods Enzymol. 24 B*, 123−134.
60. Messinger, J. (1993) Ph.D. Thesis, TU Berlin, Berlin.
61. Nugent, J. H. A., Demetriou, C., and Lockett, C. J. (1987) *Biochim. Biophys. Acta 894*, 534−542.
62. Vass, I., Deak, Z., Jegerschold, C., and Styring, S. (1990) *Biochim. Biophys. Acta 1018*, 41−46.
63. Messinger, J., and Renger, G. (1993) *Biochemistry 32*, 9379−9386.
64. Seeliger, A. G., Kurreck, J., and Renger, G. (1997) *Biochemistry 36*, 2459−2464.
65. Renger, G., Eckert, H. J., Hagemann, R., Hanssum, B., Koike, H., and Wacker, U. (1989) in *Photosynthesis: Molecular Biology and Bioenergetics* (Singhal, G. S., Barber, J., Dilley, R. A., Govindjee, Haselkorn, R., and Mohanty, P., Eds.) pp 357−371, Narosa Publishing House, New Delhi.
66. Lavorel, J. (1976) *J. Theor. Biol. 57*, 171−185.
67. Christen, G., Reifarth, F., and Renger, G. (1998) *FEBS Lett. 429*, 49−52.
68. Schilstra, M. J., Rappaport, F., Nugent, J. H. A., Barnett, C. J., and Klug, D. R. (1998) *Biochemistry 37*, 3974−3981.
69. Christen, G., and Renger, G. (1999) *Biochemistry 38*, 2068−2077.
70. Messinger, J., Robblee, J. H., Bergmann, U., Fernandez, C., Glatzel, P., Visser, H., Cinco, R. M., McFarlane, K. L., Bellacchio, E., Pizarro, S. A., Cramer, S. P., Sauer, K., Klein, M. P., and Yachandra, V. K. (2001) *J. Am. Chem. Soc. 123*, 7804−7820.
71. Shinkarev, V. P. (1996) *Photosynth. Res. 48*, 411−417.
72. Boerner, R. J., Bixby, K. A., Nguyen, A. P., Noren, G. H., Debus, R. J., and Barry, B. A. (1993) *J. Biol. Chem. 268*, 1817−1823.
73. Faller, P., Debus, R. J., Brettel, K., Sugiura, M., Rutherford, A. W., and Boussac, A. (2001) *Proc. Natl. Acad. Sci. U.S.A. 98*, 14368−14373.
74. Christen, G., Seeliger, A., and Renger, G. (1999) *Biochemistry 38*, 6082−6092.
75. Garbers, A., Reifarth, F., Kurreck, J., Renger, G., and Parak, F. (1998) *Biochemistry 37*, 11399−11404.
76. Reifarth, F., and Renger, G. (1998) *FEBS Lett. 428*, 123−126.
77. Jeans, C., Schilstra, M. J., Ray, N., Husain, S., Minagawa, J., Nugent, J. H. A., and Klug, D. R. (2002) *Biochemistry 41*, 15754−15761.
78. Delrieu, M. J. (1983) *Z. Naturforsch. C 38*, 247−258.

BI034744B